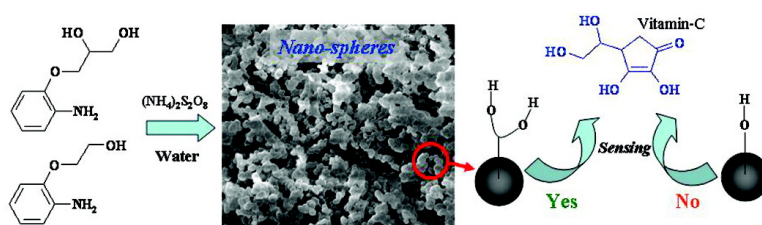


Hydroxyl-Functionalized Polyaniline Nanospheres: Tracing Molecular Interactions at the Nanosurface via Vitamin C Sensing

P. Anilkumar, and M. Jayakannan

Langmuir, 2008, 24 (17), 9754-9762 • DOI: 10.1021/la801128j • Publication Date (Web): 05 August 2008

Downloaded from <http://pubs.acs.org> on February 13, 2009



More About This Article

Additional resources and features associated with this article are available within the HTML version:

- Supporting Information
- Access to high resolution figures
- Links to articles and content related to this article
- Copyright permission to reproduce figures and/or text from this article

[View the Full Text HTML](#)



ACS Publications
High quality. High impact.

Hydroxyl-Functionalized Polyaniline Nanospheres: Tracing Molecular Interactions at the Nanosurface via Vitamin C Sensing

P. Anilkumar[†] and M. Jayakannan^{*‡}

Chemical Sciences & Technology Division, National Institute for Interdisciplinary Science and Technology (NIIST), Thiruvananthapuram 695019, Kerala, and Department of Chemistry, Indian Institute of Science Education and Research (IISER), NCL Innovation Park, Dr. Homi Bhabha Road, Pune 411008, India

Received April 10, 2008. Revised Manuscript Received June 23, 2008

Here, we report a synthesis of novel polyaniline nanospheres bearing mono- and bishydroxyl functional groups to trace the molecular interactions at the nanosurfaces through vitamin C sensing. Two new aniline monomers were synthesized via a tailor-made approach and polymerized to produce soluble and uniform polyaniline nanospheres. The structures of the monomers and polymers were characterized by NMR, FT-IR, and MS techniques, and the morphology of the nanomaterials was analyzed by SEM and TEM. The mechanistic aspects of the nanomaterial formations were analyzed by FT-IR and dynamic light scattering techniques. These studies revealed that the hydroxyl-functionalized monomers have strong hydrogen bonding at the monomer level and form spherical aggregates in water, which are templates for the polyaniline nanospheres 600 ± 100 nm in size. A controlled synthesis was also carried out using aniline hydrochloride as an unsubstituted counterpart, which yields polyaniline nanofibers. WXR analysis confirmed the presence of a sharp peak at lower angle at $2\theta = 7.3^\circ$ (d -spacing of 13.4 Å) in hydroxyl-substituted nanospheres with respect to enhancement of solid-state ordered crystalline domains, whereas unsubstituted nanofibers were found to be highly amorphous. Vitamin C was employed as an analyte to trace the molecular interaction at the nanosphere surface and study the influence of nanosurface functionalization on the sensing ability of biomolecules. The bishydroxyl-functionalized polyaniline nanospheres were found to show efficient molecular interactions toward vitamin C, whereas nanospheres with a monohydroxyl group or unsubstituted nanofibers failed as sensing materials. In a nut shell, in the present investigation, for the first time, we have proved the importance of surface functionalization of polyaniline nanomaterial, exclusively nanospheres, using hydroxyl groups for studying the molecular interactions at the nanosurfaces with biomolecules such as vitamin C.

Introduction

Polyaniline nanomaterials have been widely studied for electronic and optical applications because of their simple and reversible acid–base doping–dedoping chemistry, which enables control over properties such as electrical conductivity and optical properties.¹ These electrically conducting nanostructures have found potential applications in chemical sensors,² optoelectronic devices,³ energy storage systems,⁴ and self-cleaning surface coatings.⁵ Polyaniline nanowires or nanofibers have been synthesized using hard or soft templates by various approaches such as emulsion,^{6–8} interfacial methods,⁹ rapid mixing,¹⁰ and dilute polymerization,¹¹ etc. Though a large number of methods are known for the synthesis of nanofibers, the synthesis of

nanospheres is a challenging task mainly because the nanofibrillar morphology appears to be intrinsic to polyaniline while synthesized in water.¹² Unlike that of polyaniline nanofibers, the use of polyaniline nanospheres is restricted due to this synthetic limitation and because most of the properties of the nanospheres are not completely understood. The nanospheres are particularly interesting for optoelectronics and sensors due to their large surface area compared to that of the nanofibers. It is also important to note that the nanospheres can be effectively solvated due to their globular nature, which enhances the solubility in common solvents for structural characterization by spectroscopic techniques.¹³ There are very few examples reported for the synthesis of polyaniline nanospheres, which include using templates such as polystyrene spheres¹⁴ and hydroxy alkyl cellulose¹⁵ and salicylic acid assisted polymerization,¹⁶ etc. Recently we have reported polyaniline nanospheres (also fibers and tubes) based on a renewable resource based amphiphilic azobenzenesulfonic acid as a dopant via an interfacial route.^{17–20} However, it was found that the nanosphere formation is highly sensitive to the dopant/aniline and polymerization route, and in general, the synthesis and mechanism of nanosphere formation were not understood unlike its nanofiber counterparts.¹⁸ Here, we have

* To whom correspondence should be addressed. E-mail: jayakannan@iiserpune.ac.in. Fax: 0091-20-25898022.

[†] NIIST.

[‡] IISER.

(1) Skotheim, T. A.; Elsenbaumer, R. L.; Reynolds, J. R. *Handbook of Conducting Polymers*, 2nd ed.; Marcel Dekker: New York, 1997.

(2) Huang, J.; Virji, S.; Weiller, B. H.; Kaner, R. B. *Chem.—Eur. J.* **2004**, *10*, 1314.

(3) Alam, M. M.; Wang, J.; Guo, Y.; Lee, S. P.; Tseng, H. R. *J. Phys. Chem. B.* **2005**, *109*, 12777–12784.

(4) Zhang, X.; Goux, J. W.; Manohar, S. K. *J. Am. Chem. Soc.* **2004**, *126*, 4502–4503.

(5) Chiou, N. R.; Lu, C.; Guan, J.; Lee, L. J.; Epstein, A. *J. Nat. Nanotechnol.* **2007**, *2*, 354–357.

(6) Qiu, H.; Zhai, J.; Li, S.; Jiang, L.; Wan, M. *Adv. Funct. Mater.* **2003**, *13*, 925–928.

(7) Yan, Y.; Yu, Z.; Huang, Y. W.; Yuan, W. X.; Wei, Z. X. *Adv. Mater.* **2007**, *19*, 3353–3357.

(8) Han, J.; Song, G.; Guo, R. *Adv. Mater.* **2007**, *19*, 2993.

(9) Huang, J.; Virji, S.; Weiller, B. H.; Kaner, R. B. *J. Am. Chem. Soc.* **2003**, *125*, 314.

(10) Huang, J.; Kaner, R. B. *Angew. Chem., Int. Ed.* **2004**, *43*, 5817–5821.

(11) Chiou, N. R.; Epstein, A. *J. Adv. Mater.* **2005**, *17*, 1679–1683.

(12) Huang, J.; Kaner, R. B. *Chem. Commun.* **2006**, 367, n/a.

(13) Jin, E.; Wang, X.; Liu, N.; Zhang, W. *Mater. Lett.* **2007**, *61*, 4959–4962.

(14) Barthet, C.; Armes, S. P.; Lascelles, S. F.; Luk, S. Y.; Stanley, H. M. E. *Langmuir* **1998**, *14*, 2032–2041.

(15) Riede, A.; Helmstedt, M.; Riede, V.; Stejskal, J. *Langmuir* **1998**, *14*, 6767–6771.

(16) Zhang, L.; Wan, M. X. *Adv. Funct. Mater.* **2003**, *13*, 815–820.

(17) Anilkumar, P.; Jayakannan, M. *Langmuir* **2006**, *22*, 5952–5957.

(18) Anilkumar, P.; Jayakannan, M. *J. Phys. Chem. C* **2007**, *111*, 3591–3600.

(19) Anilkumar, P.; Jayakannan, M. *Macromolecules* **2007**, *40*, 7311–7319.

(20) Jinish Antony, M.; Jayakannan, M. *J. Phys. Chem. B* **2007**, *111*, 12772–12780.

attempted to develop an alternate approach for nanospheres based on a functionalized aniline monomer with hydroxyl groups. This approach is very attractive mainly because the resultant nanomaterials bear functional groups at the nanosphere surface which can be employed as tools for trapping various chemical and biological analytes for sensing applications. Though polyanilines (not nanomaterials) with functional groups such as alkyl,²¹ sulfonic acids,²² mesogenic groups,²³ and halide²⁴ at the ortho position in the aromatic ring have been reported in the literature, so far polyaniline nanomaterials with active functional groups have not been explored.

Here, we report the synthesis of novel polyaniline nanospheres bearing mono and bishydroxyl functional groups to study the molecular interactions at the nanosurfaces via vitamin C sensing. Two new aniline monomers were synthesized with hydroxyl groups and polymerized via an oxidative route to produce water-soluble and uniform nanospheres. The structures of the monomers and polymers were characterized by NMR, FT-IR, and MS techniques, and the morphology of the nanomaterials was analyzed by SEM and TEM. FT-IR revealed that the hydroxyl-functionalized monomers have strong hydrogen-bonding interaction at the monomer level. Dynamic light scattering experiments of the monomers in water revealed that the monomers form a sub-micrometer size aggregate in water which is a selective template for polyaniline nanospheres rather than nanofibers. The hydroxyl functionality also improves solvent-particle interactions and the solubility of the polymer in various solvents such as water and dimethyl sulfoxide, which eases the structural characterization by NMR and other spectroscopic techniques [generally, polyaniline nanomaterials are not characterized by NMR and other techniques due to their poor solubility]. A controlled experiment with an unsubstituted aniline monomer (aniline hydrochloride) resulted in the formation of polyaniline nanofibers, confirming the importance of the hydroxyl group in the aniline monomer for producing nanospheres. To study the influence of nanosurface functionality on the sensing behavior, interactions of vitamin C with nanospheres having mono- or bishydroxyl groups (also without functional groups) were carried out in water. The primary idea of the work is not to develop a powerful vitamin C sensor but to study and understand the molecular interactions at the nanomaterial surface. The studies revealed that the nanospheres with bishydroxyl groups have high-level sensing compared to that of nanospheres with a monohydroxyl or nanofibers without any functional groups. In a nut shell, in the present approach, we have demonstrated that the functionalization of aniline with hydroxyl groups produces exclusively polyaniline nanospheres (no nanofibers) and the hydroxyl groups at the nanosurface are very essential for sensing of bioanalytes such as vitamin C.

Experimental Section

Materials. 2-Aminophenol, aniline hydrochloride salt (AHC), 3-chloro-1,2-propanediol, 2-chloroethanol, ammonium persulfate (APS), vitamin C, hydrochloric acid, and sodium hydroxide were purchased locally and purified by following standard procedures.

Measurements. NMR spectra of the compounds were recorded using a 300 MHz Bruker NMR spectrophotometer. Infrared spectra of the polymers were recorded using a Perkin-Elmer Spectrum One, FT-IR spectrophotometer in the range from 4000 to 400 cm^{-1} . The purity of the compounds was determined by fast atom bombardment (FAB) high-resolution mass spectrometry (JEOL JSM600 instru-

ment). For SEM measurements, the polymer samples were given a thin gold coating using a JEOL JFC-1200 fine coater. The probing side was inserted into a JEOL JSM- 5600 LV scanning electron microscope for taking photographs. Wide-angle X-ray diffraction of the finely powdered polymer samples was recorded with a Philips Analytical diffractometer using $\text{Cu K}\alpha$ emission. The spectra were recorded in the range of $2\theta = 0-50^\circ$ and analyzed using X'Pert software. UV-vis spectra of the PANI in water were recorded using a Perkin-Elmer Lambda-35 UV-vis spectrophotometer. All the polymers were dedoped using aqueous ammonia, washed well with deionized water, and dried. The predried powder was dispersed in water under ultrasonic stirring to get a solution with an absorbance of 0.3 (OD) (for sensing studies). Transmission electron microscopy images were recorded using an FEI Tecnai 30G² S Twin HRTEM instrument at 100 kV. For TEM measurements, the water suspension of the nanospheres was prepared under ultrasonic stirring and deposited on a Formvar-coated copper grid. For dynamic light scattering (DLS) measurements, we used a Nano ZS Malvern instrument employing a 4 mW He-Ne laser ($\lambda = 632.8 \text{ nm}$) and equipped with a thermostated sample chamber. For conductivity measurements, the polymer samples were pressed into a 10 mm diameter disk and were measured by a standard four-probe method using a Keithley 6881 programmable current source and 2128A nanovoltmeter at 30 °C. The resistivity of the samples was measured at five different positions, and at least two pellets were measured for each sample: the average of 10 readings was used for conductivity calculations.

Synthesis of 2-Hydroxyacetanilide (1). 2-Aminophenol (11.0 g, 0.1 mol) was suspended in water (30 mL) by magnetic stirring. Acetic anhydride (12 mL, 0.13 mol) was added, and the entire mixture was warmed to 70 °C for 3 h with constant stirring. The mixture was cooled, and the precipitate was filtered, washed with water, and dried in a vacuum oven at 50 °C. The crude solid was further purified by recrystallization from warm ethanol. Yield: 10.5 g (70%). ¹H NMR (DMSO-*d*₆, 300 MHz): δ (ppm) 2.11 (s, 3H, -COCH₃), 6.85 (m, 3H, Ar H), 7.65 (d, 1H, Ar H), 9.31 (br, 1H, -NH). FT-IR (KBr, cm^{-1}): 3520, 3401, 2882, 1659, 1595, 1541, 1453, 1387, 1282, 1240, 1033, 761, 668. FAB-MS (MW 151.17): $m/z = 152.32$ (M + 1).

Synthesis of 2-(2,3-Dihydroxypropoxy)acetanilide (2). Sodium hydroxide (5.6 g, 0.14 mol) was dissolved in a 50 mL ethanol + water mixture (1:1, v/v). 2-Hydroxyacetanilide (10.6 g, 0.07 mol) was added to the sodium hydroxide solution and the resulting solution refluxed for 1 h. The solution was cooled, 3-chloro-1,2-propanediol (15.5 g, 0.14 mol) was added, and the resulting solution was refluxed for 35 h. The slow evaporation of ethanol at atmospheric pressure resulted in the precipitation of the product as a white solid. The precipitate was filtered, washed with acetone, and dried in a vacuum oven at 50 °C. The crude product was further purified by recrystallization from hot ethanol. Yield: 11.8 g (70%). ¹H NMR (DMSO-*d*₆, 300 MHz): δ (ppm) 2.1 (s, 3H, aliphatic H), 3.8 (t, 2H, -OCH₂), 4.06 (d, 2H, -OCH₂), 4.77 (d, 1H, -OC*H), 5.2 (d, 1H, -OC*H), 6.9 (br, 1H, Ar H), 7.01 (br, 2H, Ar H), 8.02 (d, 1H, Ar H), 9.08 (s, 1H, -NH). FT-IR (KBr, cm^{-1}) 3351, 3272, 2944, 2881, 1654, 1539, 1460, 1255, 1050, 963, 784, 676, 605. FAB-MS (MW 225.25): $m/z = 226.21$ (M + 1).

Synthesis of 2-(2-Hydroxyethoxy)acetanilide (3). 2-Hydroxyacetanilide (10.6 g, 0.07 mol) in sodium hydroxide (5.6 g, 0.14 mol) solution was reacted with 2-chloroethanol (11.3 g, 0.14 mol) as described for 2. The product was further purified by silica gel column chromatography (50:50 ethyl acetate and hexane). Yield: 6.3 g (46%). ¹H NMR (CDCl₃, 300 MHz): δ (ppm) 2.1 (s, 3H, aliphatic H), 3.879 (t, 2H, -OCH₂), 4.05 (t, 2H, -OCH₂), 6.94 (t, 1H, Ar H), 6.87 (t, 1H, Ar H) 6.82 (d, 1H, Ar H), 8.15 (br, 2H, Ar H, -NH). FT-IR (KBr, cm^{-1}): 3330, 2935, 2870, 1677, 1601, 1535, 1488, 1447, 1370, 1323, 1288, 1251, 1210, 1123, 1080, 1045, 909, 750, 602, 543. FAB-MS (MW 195.22): $m/z = 196.20$ (M + 1).

Synthesis of 2-(2,3-Dihydroxypropoxy)aniline Hydrochloride (4). 2 (1.5 g, 0.006 mol) was dissolved in ethanol (20 mL), concentrated HCl (10 mL) was added, and the resulting solution was refluxed for 30 h under a nitrogen atmosphere. The solution was

(21) Zaidi, N. A.; Foreman, J. P.; Tzamalidis, G.; Monkman, S. C.; Monkman, A. P. *Adv. Funct. Mater.* **2004**, *14*, 479-486.

(22) Chen, S. A.; Hwang, G. W. *J. Am. Chem. Soc.* **1994**, *116*, 7939-7940.

(23) Goto, H.; Akagi, K. *Macromolecules* **2002**, *35*, 2545-2551.

(24) Kwon, H.; Conklin, J. A.; Makhinson, M.; Kaner, R. B. *Synth. Met.* **1997**, *84*, 95-96.

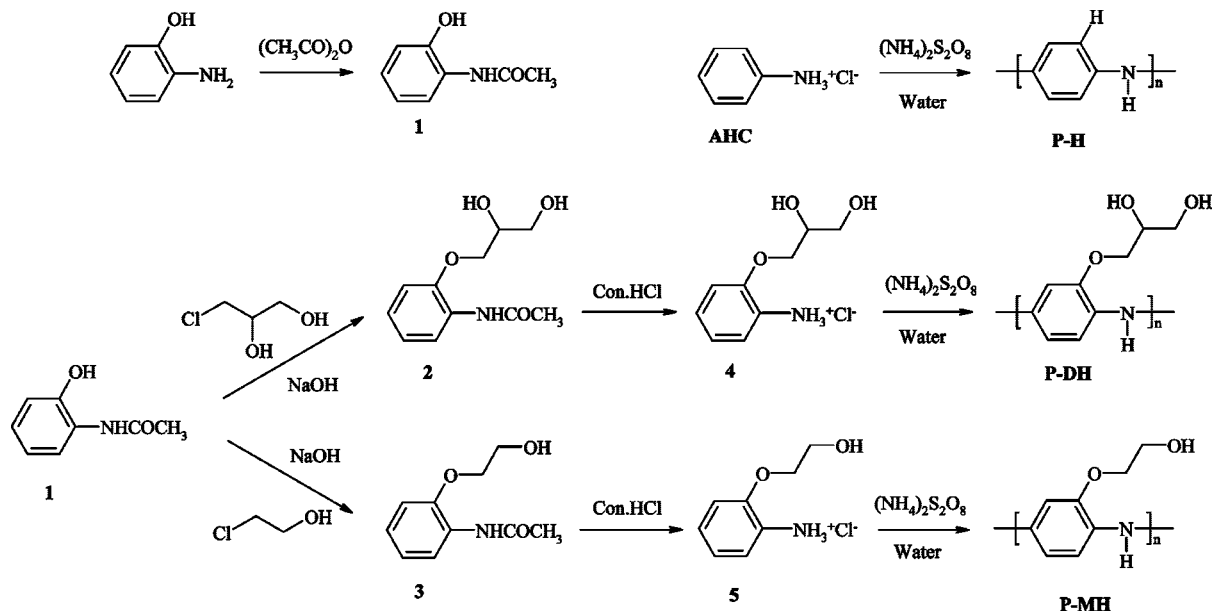


Figure 1. Synthesis of hydroxyl-functionalized polyaniline nanomaterials.

cooled, and ethanol was removed by rotary evaporation. Upon being allowed to stand in a freezer, the viscous liquid crystallized out. The crystallized product was washed with acetone and dried in an oven at 60 °C. The crude solid was purified by recrystallization from water. Yield: 0.97 g (80%). $^1\text{H NMR}$ (D_2O , 300 MHz): δ (ppm) 3.8 (br, 2H, $-\text{OCH}_2$), 3.96 (br, 2H, $-\text{OCH}_2$), 4.15 (br, 2H, $-\text{OCH}_2$), 7.01 (t, 1H, Ar H), 7.18 (d, 1H, Ar H), 7.37 (m, 2H, Ar H), 10.2 (br, 2H, NH_3^+). $^{13}\text{C NMR}$ (D_2O , 75 MHz): δ (ppm) 39.5, 62.2, 69.8, 71.1, 113.1, 120.8, 123.9, 129.3, 151.7. FT-IR (KBr, cm^{-1}): 3225, 2860, 2620, 2034, 1632, 1502, 1446, 1327, 1265, 1163, 1101, 1051, 979, 942, 846, 755, 646, 506. FAB-MS (MW 183.21): $m/z = 184.43$ ($\text{M} + 1$).

Synthesis of 2-(2-Hydroxyethoxy)aniline Hydrochloride (5). **3** (3 g, 0.015 mol) was dissolved in ethanol and the resulting solution treated with concentrated HCl as described for **4**. The crude solid was purified by recrystallization from water. Yield: 1.5 g (65%). $^1\text{H NMR}$ (D_2O , 300 MHz): δ (ppm) 3.75 (t, 2H, $-\text{OCH}_2$), 4.1 (t, 2H, $-\text{OCH}_2$), 7.01 (t, 1H, Ar H), 7.18 (d, 1H, Ar H), 7.31 (m, 1H, Ar H), 7.39 (m, 1H, Ar H), 9.85 (br, 2H, NH_3^+). $^{13}\text{C NMR}$ (D_2O , 75 MHz): δ (ppm) 39.5, 59.4, 70.7, 113.1, 120.8, 123.7, 129.1, 151.5. FT-IR (KBr, cm^{-1}): 3348, 2866, 2612, 2010, 1641, 1542, 1502, 1455, 1321, 1296, 1265, 1190, 1128, 1066, 1044, 917, 895, 852, 761, 606, 550, 503. FAB-MS (MW 153.18): $m/z = 154.33$ ($\text{M} + 1$).

Synthesis of Poly[2-(2,3-dihydroxypropoxy)aniline] (P-DH). Monomer **4** (1.09 g, 0.005 mol) was dissolved in water (15 mL) and the solution oxidized by ammonium persulfate (1.25 g, 0.0055 mol) in water (15 mL). The reaction mixture was kept for 24 h without disturbance at room temperature. The precipitate was centrifuged and washed several times with water and methanol. The isolated mass was dried in a vacuum oven at 55 °C for 40 h. Yield: 0.46 g (43%). $^1\text{H NMR}$ ($\text{DMSO}-d_6$, 300 MHz): δ (ppm) 6.9 (1H, Ar H), 7.07 (1H, Ar H), 7.24 (1H, Ar H). FT-IR (cm^{-1}): 3414, 3197, 2934, 1572, 1485, 1414, 1336, 1268, 1182, 1101, 996, 829, 789, 674, 612, 584, 504.

A similar procedure was adapted to synthesis P-MH from **5**. Yield: 45%. $^1\text{H NMR}$ ($\text{DMSO}-d_6$, 300 MHz): δ (ppm) 6.95 (1H, Ar H), 7.12 (1H, Ar H), 7.3 (1H, Ar H). FT-IR (cm^{-1}): 3202, 2935, 1574, 1485, 1266, 1195, 1112, 1035, 988, 899, 811, 610, 586. Aniline hydrochloride was polymerized as described above to prepare P-H. Yield: 92%. FT-IR (cm^{-1}): 3191, 1564, 1478, 1301, 1243, 1107, 881, 802, 703, 617, 588, 502. Insoluble for NMR characterization.

Results and Discussion

Two monomers consisting of hydroxyl functional groups in aniline at the ortho position were synthesized as shown in Figure

1. The reactive amine group in 2-hydroxyaniline was protected by acetylation using acetic anhydride to yield 2-hydroxyacetanilide (**1**). **1** was reacted with 3-chloro-1,2-dihydroxypropane and 2-chloroethanol under Williamson's etherification in ethanol/water to yield **2** or **3**. Subsequently, **2** and **3** were treated with concentrated HCl at 60 °C to remove the acetyl protecting group, resulting in the formation of amine hydrochloride salts **4** and **5**, respectively. Compounds **4** and **5** were purified by recrystallization from hot water to get pure white crystals. Typically, 1 g of monomer **4** (or **5**) was dissolved in 15 mL of doubly distilled water and the solution oxidized with ammonium persulfate (0.36 M) solution in water. The polymerization was continued for 24 h without disturbance at room temperature (30 °C). The room temperature polymerization was adapted for nanomaterial synthesis from the novel hydroxyl-functionalized monomers because the kinetics of polymerization is relatively high at 30 °C compared to 0–5 °C (usual temperature for conventional polymerization), and under these condition homogeneous nucleation favors the formation of uniform nanostructures.²⁵ The product was filtered and washed with a large amount of water followed by methanol till the filtrate became colorless. Two polyaniline nanomaterials, P-DH and P-MH (DH and MH refer to dihydroxyl and monohydroxyl), were prepared from monomers **4** and **5**, respectively (see Figure 1). To study the influence of hydroxyl groups on the morphology and other physicochemical properties of polyaniline nanomaterials, a controlled polyaniline sample (P-H) was synthesized using aniline hydrochloride (AHC) as the monomer under identical experimental conditions (see Figure 1). P-H was synthesized from AHC in water instead of conventional aniline in an acidic medium²⁵ because the other two monomers, **4** and **5**, were amine hydrochloride salts and polymerized under neutral conditions. This enables us to study the effect of hydroxyl substitution on the structure–property relationship of all three polymers under identical conditions without the influence of an external dopant such as HCl. The structures of the monomers and polymers were confirmed by $^1\text{H NMR}$, FTIR, and MS. $^1\text{H NMR}$ spectra of the monomers are shown in Figure 2, and various types of protons in the structures are assigned alphabetically. Both the monomers showed aliphatic protons of the $-\text{OCH}_2$ group in the 3–4 ppm region and aromatic

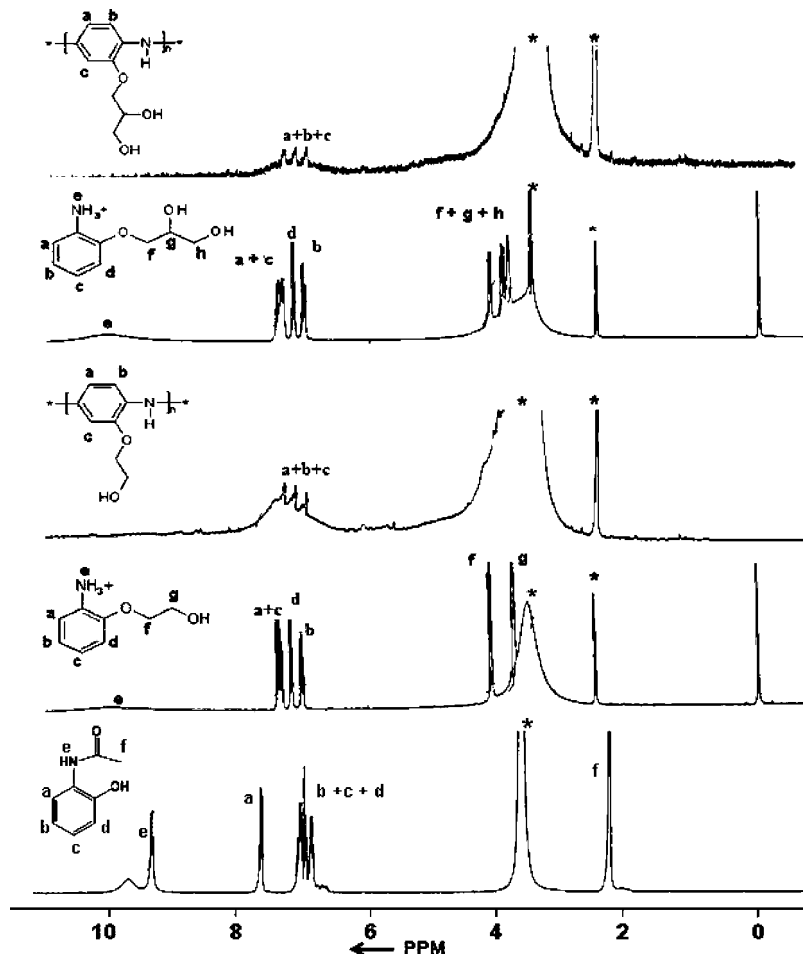


Figure 2. ^1H NMR spectra of the hydroxy monomers and the corresponding polyaniline nanospheres in $\text{DMSO-}d_6$.

Table 1. Yield, Inherent Viscosity, Conductivity, Dimensions, and WXR D Data of Polyaniline Nanomaterials

| sample | yield (%) | η_{inh}^a (dL/g) | σ^b (S/cm) | diameter ^c (nm) | peaks in WXR D ^d | |
|--------|-----------|------------------------------|----------------------|----------------------------|-----------------------------|------------------|
| | | | | | 2θ (deg) | d -spacing (Å) |
| P-DH | 43 | 0.58 | 2.8×10^{-3} | spheres, 700 ± 100 | 6.8, 20.6, 24.4 | 13.1, 4.3, 3.6 |
| P-MH | 45 | 0.45 | 4.6×10^{-3} | spheres, 600 ± 150 | 7.3, 24.4 | 13.4, 3.6 |
| P-H | 92 | 0.66 | 2.5×10^{-1} | fibers, ~ 50 | 25.6, 29.7 | 3.1, 2.1 |

^a Inherent viscosity measured at 30 °C using an Ubbelohde viscometer. ^b Measured using four-probe conductivity set up at 30 °C. ^c The average diameter is calculated on the basis of SEM images. ^d Wide-angle X-ray diffraction measurements were carried out at 30 °C.

protons in the 6–9 ppm region. The monomers also showed a less intense broad peak at ~ 10 ppm, which originates from ammonium ion (NH_3^+) protons.²³ One of the limitations of conventional polyaniline is its poor solubility in common organic solvents, which hampered the structural characterization by NMR. Interestingly, the presence of hydroxyl groups in the polymers made these samples soluble in highly polar solvents such as DMSO (also DMF), which enabled us to record their NMR spectra. The NMR spectra of both polymers were recorded in $\text{DMSO-}d_6$ and are shown in Figure 2. Three aromatic protons in the polyaniline unit appear as sharp peaks in the 6.8–7.4 ppm region.²³ The disappearances of the para (to the amine group) aromatic proton and the absence of a signal at 10.15 ppm corresponding to $-\text{NH}_3^+$ (visible in the monomer spectrum) in the polymer spectrum confirmed the formation of the expected polymer structures. The protons of the side chain methylene groups are expected to appear at 3.5–4.5 ppm, but these peaks are unable to be distinguished since they are merged with the solvent peaks (water, DMSO). The polymer P-H without hydroxyl

functionalization (prepared from anilinium hydrochloride) is not soluble in DMSO, which restricts its structural characterization by NMR. The molecular weights of P-DH and P-MH were determined by the viscosity method in DMSO at 30 °C using an Ubbelohde viscometer for 0.5 wt % polymer samples. The solubility of the P-H sample was very low in DMSO, and therefore, only a 0.3 wt % solution was used for the measurements. The inherent viscosities were obtained as 0.58, 0.45, and 0.66 dL/g for P-DH, P-MH, and P-H, respectively (see Table 1). The inherent viscosity values match those of the polyaniline samples from earlier reports,^{26,27} which confirms that the molecular weights obtained are very good for further analysis.

The morphologies of the polyaniline nanomaterials were recorded using a JEOL JSM- 5600 LV scanning electron microscope, and SEM images of the P-DH, P-MH, and P-H

(26) Kim, B. J.; Oh, S. G.; Han, M. G.; Im, S. S. *Synth. Met.* **2001**, *122*, 297–304.

(27) Jayakannan, M.; Annu, S.; Ramalekshmi, S. *J. Polym. Sci., Part B: Polym. Phys.* **2005**, *43*, 1321–1331.

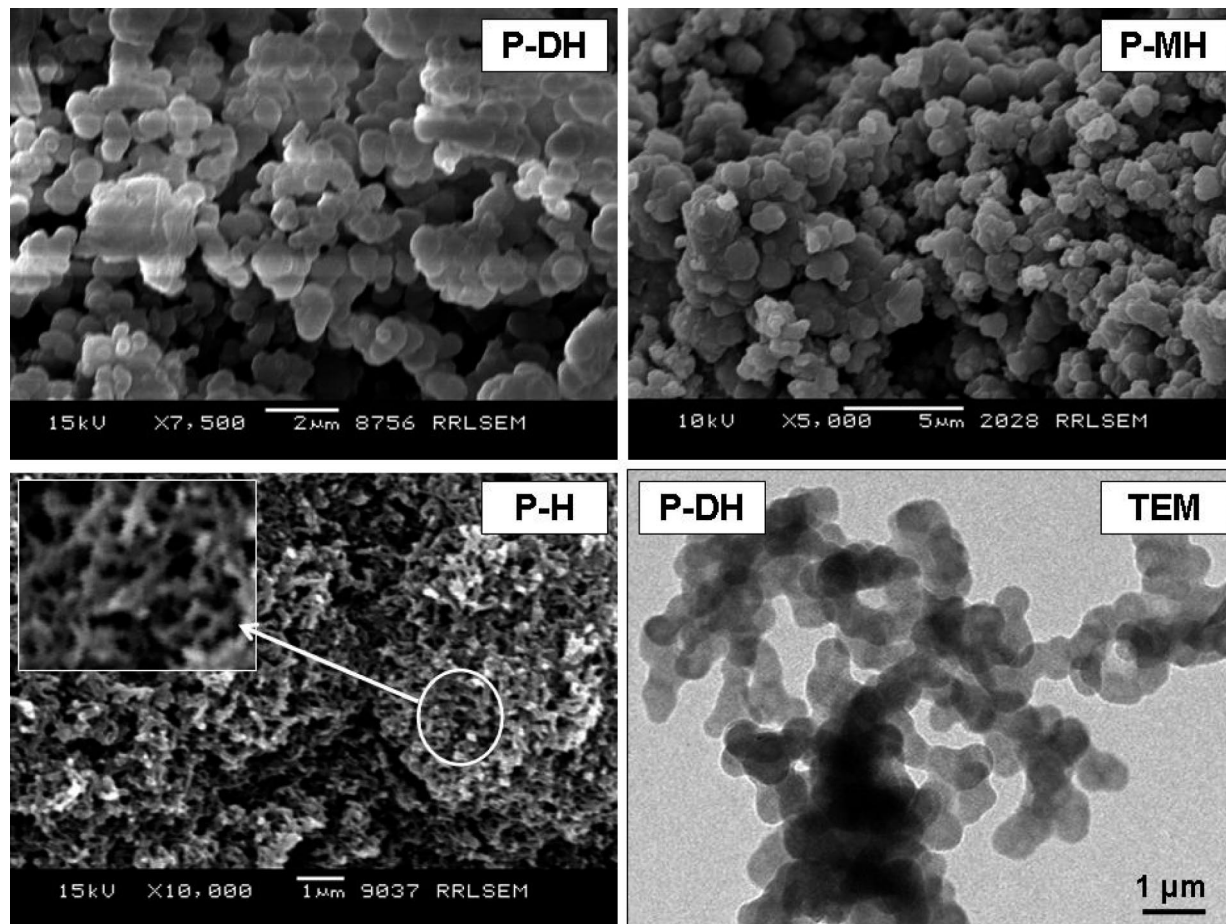


Figure 3. SEM and TEM images of polyaniline materials.

polyaniline samples are given in Figure 3. The P-DH and P-MH samples were found to be full of nanospheres and devoid of any nanofibers. P-DH contains spheres of diameter ranging from 600 to 800 nm, and they appear as a cluster. In the case of P-MH the diameters of the nanospheres range from 450 to 750 nm, and the spheres are more or less well-separated. The P-H sample (without any hydroxyl functionalization) was found to be thin nanofibers of diameter less than 50 nm, and there is no trace amount of nanospheres. For TEM analysis, the sample was dispersed in water under ultrasonic conditions, and a drop of the solution was evaporated on the Cu grid. The TEM image of P-DH (see Figure 3) has confirmed the morphology of rigid nanospheres of 500 nm diameter, which matches that of the SEM images. The morphology of the samples is clearly evident in that the hydroxyl substitutions at the aniline monomer drastically change the morphology of the resultant nanomaterials from fibers to nanospheres. The morphology of P-H (prepared from AHC salt in water) is found to be similar to that of polyaniline nanofibers produced from aniline in acidic solution (HCl).¹⁰ This suggests that the polymerization procedures adapted in the present investigation are in concordance with the literature reports on polyaniline nanomaterial synthesis. Therefore, the difference in the morphologies in the P-DH (also P-MH) and P-H samples is directly related to the difference in the polymerization mechanism of the hydroxyl-functionalized monomers (**4** and **5**) and that of AHC. All three monomers were subjected to polymerization under identical conditions, and therefore, the difference in the nanomaterial morphology is a result of the difference in the monomer interactions at the molecular level during the polymerization process.

FT-IR is a powerful tool to trace various hydrogen-bonding interactions present at the molecular level.²⁸ To understand the hydrogen-bonding interactions of the monomers and resultant polyaniline nanomaterials, FT-IR spectra of the samples were recorded and are shown in Figure 4. The peaks corresponding to the hydrogen-bonded and free N–H (or O–H) regions are expanded for simplicity, and full-range spectra are provided as Supporting Information. The monomers (**4** and **5**) and polymers (P-DH and P-MH) have both N–H and O–H groups, and the stretching frequencies of these two groups are very close and difficult to distinguish. However, the overall presence of free as well as hydrogen-bonded N–H (or O–H) groups in the materials can be correlated on the basis of their structural features. In all the samples there are two peaks present: (i) a peak at higher wavenumber (3450–3300 cm^{-1}) corresponding to antisymmetric stretching and symmetric stretching of free N–H (or O–H) groups^{29,30} and (ii) a shoulder at lower wavenumber (3240–3100 cm^{-1}) corresponding to stretching due to hydrogen-bonded N–H (or O–H) groups.³⁰ The ratio of the intensity of these two peaks directly reflects the availability of free versus hydrogen-bonded protons with respect to their structure (see Figure 4). The ratio $A_{\text{free}}/A_{\text{H-bonded}}$ (A = absorbance) was almost 5–6 times higher for the hydroxyl-functionalized monomer compared to AHC. This suggests that the free O–H and N–H groups in monomers **4** and **5** experience strong hydrogen-bonding interactions, which may

(28) Deepa, P.; Jayakannan, M. *J Polym. Sci., Part A: Polym. Chem.* **2007**, *45*, 2351–2366.

(29) Zheng, W.; Angelopoulos, M.; Epstein, A. J.; MacDiarmid, A. G. *Macromolecules* **1997**, *30*, 7634–763.

(30) Zheng, W.; Angelopoulos, M.; Epstein, A. J.; MacDiarmid, A. G. *Macromolecules* **1997**, *30*, 2953–2955.

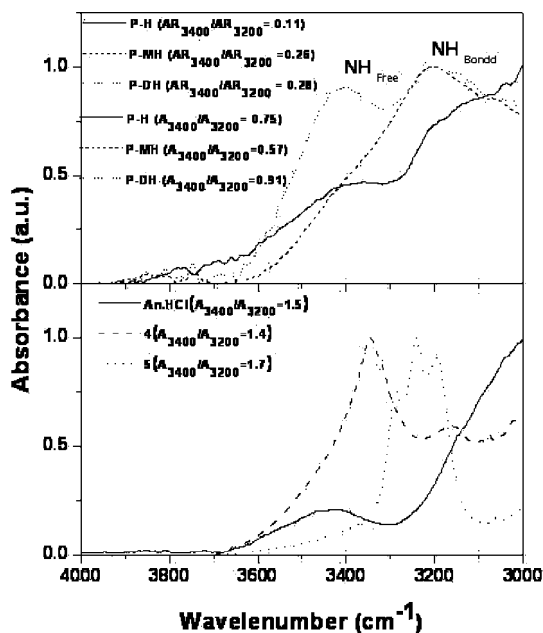


Figure 4. FT-IR spectra of polyaniline nanomaterials and monomers. AR represents the area of the peak, and A represents the absorption intensity. The plots were normalized by taking the zero absorbance at 4000 cm^{-1} in each spectrum as the baseline.

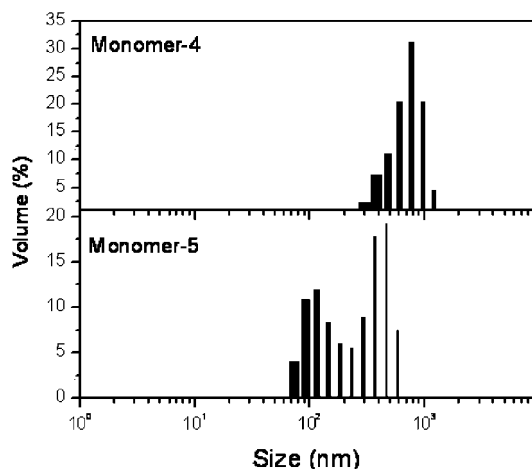


Figure 5. DLS histograms of monomers dissolved in water at $30\text{ }^{\circ}\text{C}$.

be the driving force for the nanosphere formation in the polymerization process.

Self-organization of molecules can be traced using DLS techniques in solution.³¹ DLS histograms of monomers **4** and **5** in water (0.35 M^{-1}) are shown in Figure 5. The histogram of AHC is almost featureless with a very weak and broad distribution and failed in DLS analysis; therefore, it is not included in the discussion (see the Supporting Information). The DLS plots of monomers **4** and **5** showed good distribution characteristics with aggregates of 600 and 400 nm average sizes, respectively. This suggests that the hydroxyl functional monomers undergo self-organization in water (via hydrogen bonding as evident from FT-IR analysis) to produce large submicrometer aggregates. The formation of these large aggregates is schematically shown in Figure 6. The functionalized monomer **4** (also **5**) has a water-loving hydrophilic hydroxyl head and hydrophobic aromatic ring

and behaves as an amphiphilic monomer. In water, the hydrophilic head tends to project outside and surround the aromatic ring to form a micelle. The aggregation of such small monomer micelles produces large submicrometer aggregates, which are selective templates for polyaniline nanospheres. Subsequent oxidation of these aggregated monomers by APS produces exclusively polyaniline nanospheres for hydroxyl-functionalized monomers. On the other hand, AHC did not have a selective hydrophilic/hydrophobic part in the molecular structure and resulted in the formation of nanofibers. Particle size analyses of polymer spheres are carried out in a water suspension (see the Supporting Information) at $30\text{ }^{\circ}\text{C}$. Histograms of P-DH showed a weak distribution at 50 nm (small amount) and another peak at 400 nm (large amount), whereas the P-MH sample showed a single distribution centered at 400 nm. The sizes of the nanospheres almost matched the diameters obtained from SEM data. Attempts to get good light scattering experimental data for P-H were not successful due to the poor solubility of the sample in water.

In polyaniline nanomaterials, two types of hydrogen-bonding interactions are possible: (i) hydrogen bonding among the polymer chains within the nanospheres (or nanofibers) and (ii) free N–H or O–H groups available at the periphery of the nanosurface which may undergo intermolecular hydrogen bonding at surfaces with other nanospheres (or fibers). All the samples were expected to have these two types of hydrogen bonding, but their difference in relative intensities may reflect their structural differences. To trace the hydrogen-bonding ability of nanomaterials, FT-IR spectra of the polymers were recorded (doped stage) and are shown along with those of the monomers in Figure 4. P-DH has bishydroxyl side chains and was found to have a more intense peak at 3400 cm^{-1} ($A_{\text{free}}/A_{\text{H-bonded}}$) compared to P-MH and P-H, indicating the availability of more free O–H protons at the nanosurfaces of P-DH. Additionally, the ratios of the peak areas, $AR_{\text{free}}/AR_{\text{H-bonded}}$ ($AR = \text{area of the peak}$), were obtained by the deconvolution method as 0.11, 0.27, and 0.28 for P-H, P-MH, and P-DH, respectively. It is also clear that the ratio $AR_{\text{free}}/AR_{\text{H-bonded}}$ is 2.5–3 times higher for hydroxyl polymers than the P-H polymer. P-H is more planar (no substituent), and this will help the polymer backbone undergo more π – π interactions that will make the N–H groups very close to each other, allowing them to form strong hydrogen bonds. The ratio $A_{\text{free}}/A_{\text{H-bonded}}$ was much higher for P-H compared to P-MH.³⁰ The FT-IR spectra of dedoped polymers were also recorded, and the ratios of the absorbance and peak area for free and hydrogen-bonded groups were compared (see the Supporting Information). The dedoped sample also followed a trend similar to that observed in the doped sample in both their area and intensity, which confirmed that the hydrogen-bonding nature of the nanomaterials is highly dependent on the structure rather than the doped/dedoped stage. Nevertheless, the FT-IR gives clear evidence of the availability of a large number of free hydroxyl functional groups at the surfaces of P-DH nanospheres compared P-MH nanospheres or P-H nanofibers.

To investigate the effect of a hydroxyl functionality on the solid-state crystalline characteristics of polyaniline, WXR patterns of all three polymers, P-DH, P-MH, and P-H were recorded (see Figure 7). All three samples showed characteristic Bragg diffraction peaks at $2\theta = 20^{\circ}$ and 25° , which are usually observed for polyaniline. Both P-MH and P-DH have shown a sharp peak at lower angle at $2\theta = 7.3^{\circ}$ (d -spacing of 13.4 \AA , type I emeraldine salt structure) and $2\theta = 6.8^{\circ}$ (d -spacing of 13.1 \AA), respectively.³² The appearance of the lower angle peak with a

(31) Hassan, P. A.; Raghavan, S. R.; Kaler, E. W. *Langmuir* **2002**, *18*, 2543–2548.

(32) Chiou, N. R.; Lee, L. J.; Epstein, A. J. *J. Mater. Chem.* **2008**, *18*, 2085–2089.

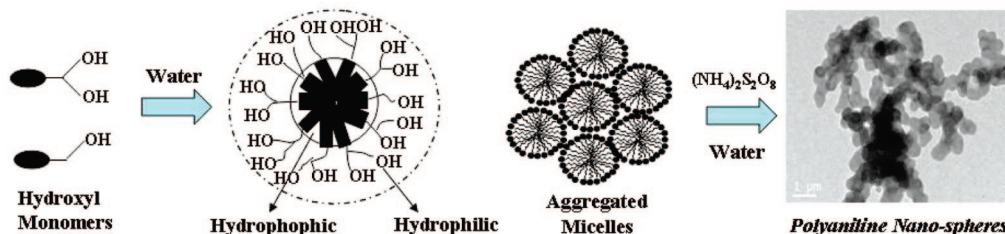


Figure 6. Plausible mechanism for the polyaniline nanosphere formation.

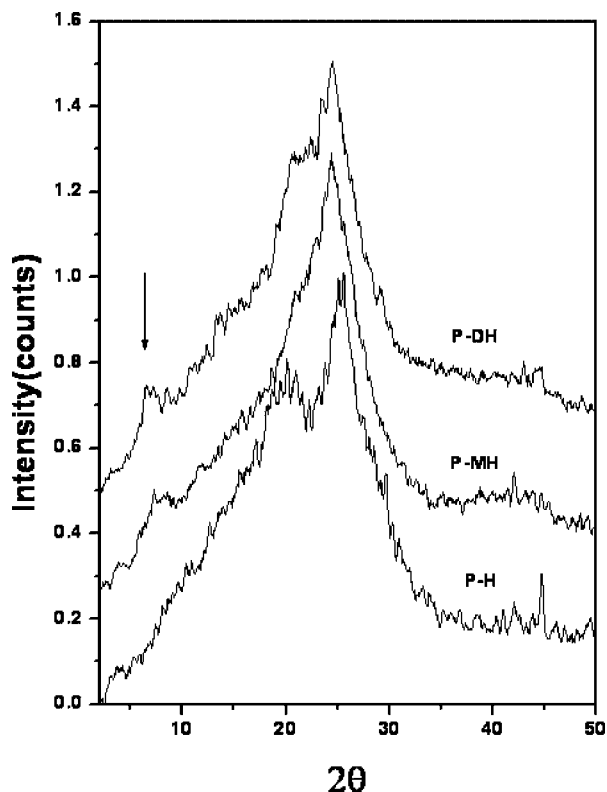


Figure 7. WXR D patterns of the nanomaterials.

high value of the d -spacing in hydroxyl-substituted polyaniline nanospheres confirmed the occurrence of enhanced solid-state ordering of polymer chains in the nanospheres compared to the nanofibers.^{33,34} In general, the solid-state ordering in the polyaniline–dopant system is enhanced by the penetration of the dopant molecules (such as CSA and an amphiphilic dopant) into the interlattice of polymer chains.^{35,17} Interestingly, in the present case, the availability of a free hydroxyl group in P-DH and P-MH enhances the solid-state ordering in the nanomaterials. The conductivity of the polyaniline nanomaterials was determined by four-probe conductivity measurement for compressed pellets at room temperature. P-H showed conductivity in the range of 2.5×10^{-1} S/cm, whereas the other nanomaterials, P-DH and P-MH, showed a lower value of the conductivity, 2.6×10^{-3} and 4.8×10^{-3} S/cm, respectively. The conductivity of P-H is 1 order lower than that of conventional doped systems (10 S/cm),⁷ which may be due to the unavailability of free acid for doping in the reaction feed. The lower conductivity of P-DH and P-MH may be due to the nonplanarity of the polymer backbone due to the steric effect induced by the side chains as reported by others.²¹ However, it is very important to note that other factors such as

the particle size and the nanomaterial shape (fibers versus spheres) may also influence the conductivity values.¹⁶

The P-DH and P-MH polymer samples were highly water dispersible owing to the hydrophilic nature of the polymer chain (P-H less soluble). The absorption spectra of the polymers in water are shown in Figure 8a. Organic solvents such as *N*-methylpyrrolidone were not employed due to the interference of dedoping of the polymer chains by the solvent molecules.³⁶ The absorption spectra of the polymers are free from a quinonoid ring (at 650 nm), which confirmed their doped nature. All three polymer samples showed three absorption maxima at approximately $\lambda = 300, 425,$ and >700 nm, which are ascribed to the $\pi-\pi^*$ transition of the benzenoid ring (300 nm) and the absorption band of the polarons.³⁷ However, their positions and relative strengths are totally different. The polaron absorption bands (approximately $\lambda = 950$ nm) for P-MH and P-H have a tail-like behavior with respect to the expanded chain conformation, whereas that of P-DH has peak characteristics corresponding to a coil-like conformation.³⁷ This suggests that, in P-DH, the phenyl rings are more twisted due to the steric effects from the side chain, resulting in a reduction in the extent of delocalization of electrons through the polymer chain. However, more detailed photophysical studies of the nanomaterials are required to confirm the conformational changes. The polyaniline nanomaterials have free and active hydroxyl groups at the nanosurfaces, and this gives opportunities to study the molecular interaction at the polyaniline nanomaterial surfaces. To trace the difference in the behavior at the nanosurfaces, a protic acid biomolecule, vitamin C (ascorbic acid), was chosen as the analyte. Recently, Bartlett et al. and Bossi et al. reported the successful sensing of vitamin C using unsubstituted polyaniline as electrode materials.^{38–40} The goal of the present investigations is not to demonstrate the efficiency of the new functionalized nanomaterial as a vitamin C sensor compared to those of the existing ones but to use it as a tool to study the molecular interaction at the nanosurfaces. Vitamin C behaves as a weak carboxylic acid⁴¹ and therefore is capable of protonating polyaniline like other dopants. It contains four hydroxyl groups and can form a hydrogen bond with the nanomaterial surface. The three types of nanomaterials are chemically different: (i) nanofibers (P-H) with N–H groups over the surface, (ii) nanospheres (P-MH) with N–H and monohydroxy groups at the surface, and (iii) nanospheres (P-DH) with bishydroxyl and N–H groups at the surface. Therefore, their interactions with vitamin C are expected to be significantly

(36) Qiu, H. J.; Wan, M. X. *J. Polym. Sci., Part A: Polym. Chem.* **2001**, *39*, 3485–3497.

(37) Xis, Y.; Wiesinger, J. M.; MacDiarmid, A. G. *Chem. Mater.* **1995**, *7*, 443–445.

(38) Bartlett, P. N.; Wallace, E. N. K. *Phys. Chem. Chem. Phys.* **2001**, *3*, 1491–1496.

(39) Bossi, A.; Castelletti, L.; Piletsky, S. A.; Turner, A. P. F.; Righetti, P. *Electrophoresis* **2003**, *24*, 3356–3363.

(40) Hanstein, S.; Bonastre, A. M.; Nestler, U.; Bartlett, P. N. *Sens. Actuators, B* **2007**, *125*, 284–300.

(41) Connell, P. J. O.; Gormally, C.; Pravda, M.; Guilbault, G. G. *Anal. Chim. Acta* **2001**, *431*, 239–247.

(33) Lunzy, W.; Banka, E. *Macromolecules* **2000**, *33*, 425.

(34) Jana, T.; Roy, S.; Nandi, A. K. *Synth. Met.* **2003**, *132*, 257.

(35) Winokur, M. J.; Guo, H.; Kaner, R. B. *Synth. Met.* **2001**, *119*, 403–404.

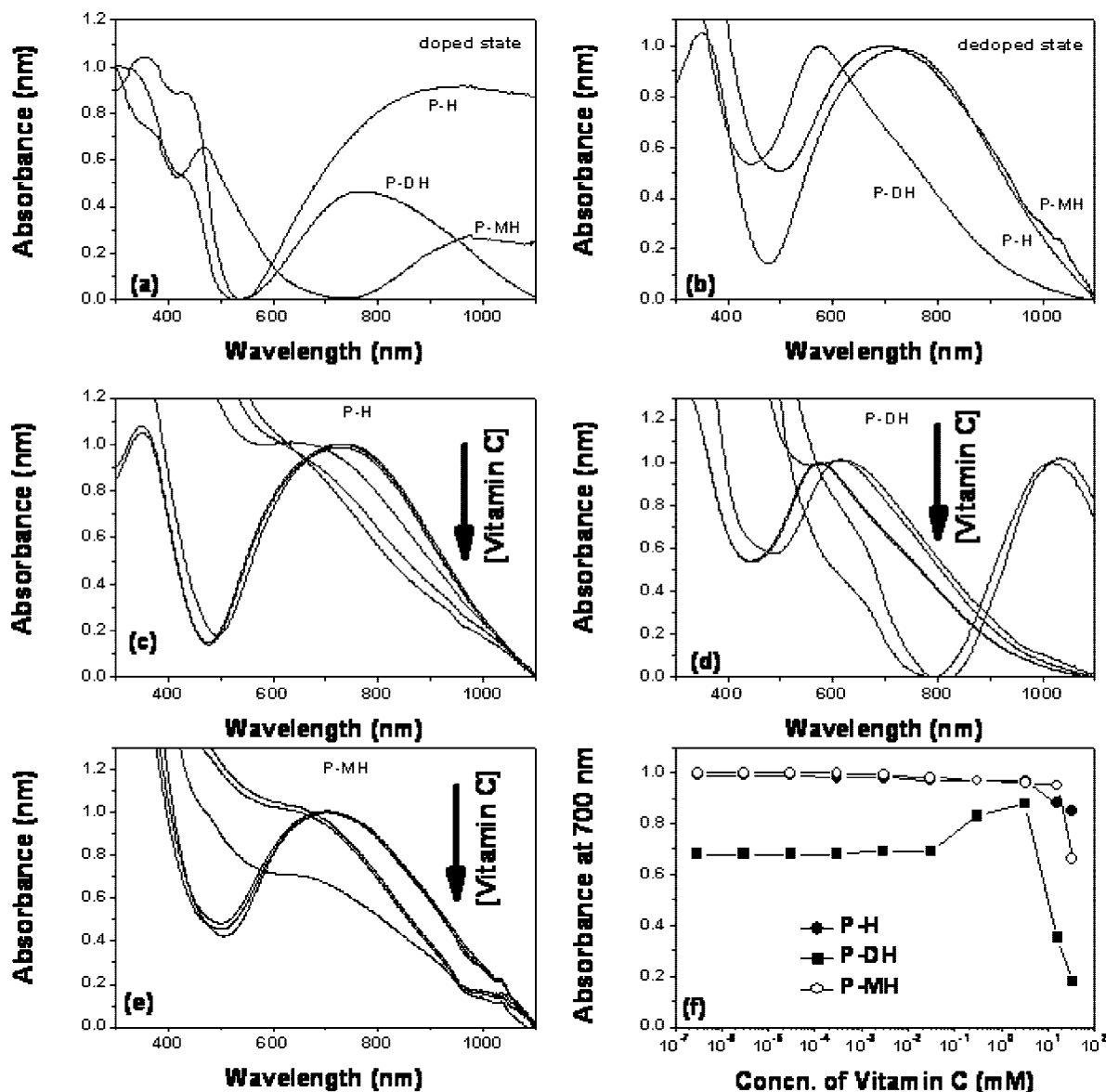


Figure 8. Normalized absorption spectra of the nanomaterials: (a) nanomaterials in water, (b) nanomaterials dedoped by aqueous ammonia. (c–f) Changes in the absorption spectra of polyaniline nanomaterials in water upon addition of vitamin C. At least two independent experiments were performed to confirm the trend in (f).

different. Various types of molecular interactions between vitamin C and nanospheres are schematically shown in Figure 9.

To trace the molecular interactions, the dedoped sample is dispersed in water with an absorbance of 0.3 (OD) (see Figure 8b). The absorbance maximum of the P-DH dedoped sample was obtained as 540 nm, which was much lower than that of 710 nm of P-MH and P-H. This suggests that the P-DH chains exist in the form of a pernigraniline base in the dedoped stage whereas the other two samples appear in the emeraldine base form.⁴² These polyaniline nanomaterial solutions are doped with ascorbic acid solutions of concentration starting from 10^{-8} to $30 \times 10^{-3} \text{ M}^{-1}$. The corresponding changes in the absorption spectra are shown in Figure 8c–e. To quantify the changes, the variation of the absorbance at 700 nm (disappearance of the quinoid ring) was plotted versus the concentration of vitamin C (see Figure 8f). The P-H and P-MH samples showed almost similar behavior toward vitamin C, and the addition of ascorbic acid did not cause a significant change in the absorbance at 700 nm in the entire

composition range. On the other hand, the dihydroxy-functionalized polyaniline nanospheres (P-DH) showed effective molecular interactions toward vitamin C for more than $1 \times 10^{-3} \text{ M}^{-1}$ concentration. This confirmed that the functional groups at the nanosurfaces have high reactivity toward the analyte (such as vitamin C). This may be a consequence of a higher oxidation state or of improved molecular interactions based on hydroxyl groups. The efficient tracing behavior of the P-DH sample toward vitamin C can be understood from the possible molecular interactions in Figure 9. The bishydroxyl functional group possesses a very unique U-shaped hydrogen-bonding socket for attracting vitamin C molecules (sites 1–3), which is not available in P-MH (or P-H). These increased hydrogen-bonding interactions help the P-DH nanospheres to attract more vitamin molecules. This will in turn help the effective doping of the polyaniline backbone of P-DH nanospheres compared with other polyaniline nanomaterials. Therefore, the interaction of vitamin C at the polyaniline nanomaterial is highly sensitive to the functional groups at the nanosurfaces. Vitamin C (or ascorbic acid) is known to be highly ionizable in water. To check the effect of pH changes

(42) Kang, E. T.; Neoh, K. G.; Tan, K. L. *Prog. Polym. Sci.* **1998**, *23*, 211–324.

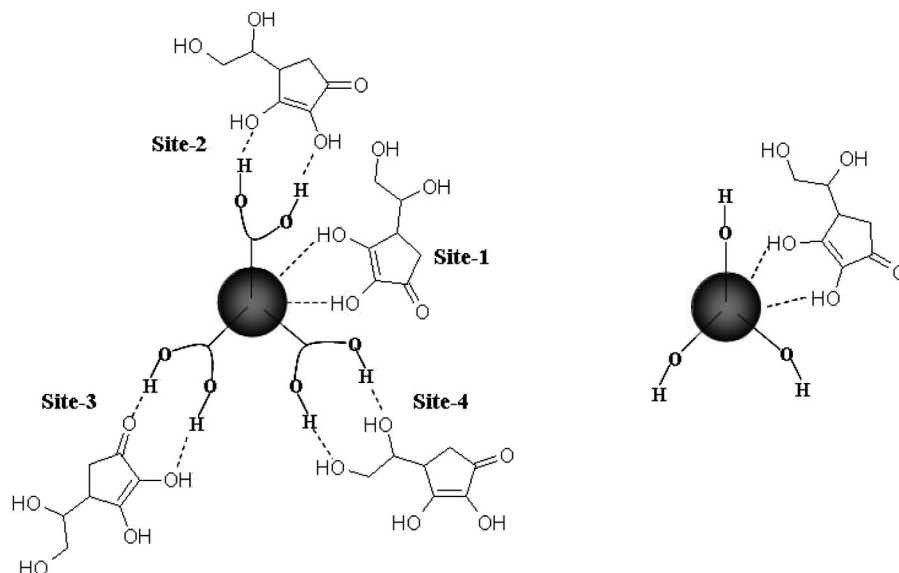


Figure 9. Scheme showing the various possible modes of interaction of vitamin C with polyaniline nanospheres.

during the doping process, first we measured the pH of the dedoped polyaniline nanomaterials solution in water (0.3 OD solution) and found the pH to be 7.05, 7.12, and 6.98 for PH, PMH, and PDH respectively. This indicates that all the solutions are neutral except the basic nature of the polymer chain, and this may be due to the low concentration of polymer samples (0.3 OD). To the dedoped sample solutions taken in separate vials was added 15 mM vitamin C, and the pH values of the solutions were checked and found to be reduced to 2.93, 2.98, and 3.14 for P-H, P-MH, and P-DH, respectively. As expected, after the addition of vitamin C the solutions became acidic, and the differences in their pH values were within the experimental error. Therefore, the difference in the sensing behavior at the nanosurface is directly correlated to the functional groups at the surface rather than other external stimuli such as the pH. In a nut shell, in the present investigation, for the first time, we have shown that the polyaniline nanomaterial, exclusively nanospheres, can be successfully functionalized using hydroxyl functional groups for tracing molecular interactions at the nanosurfaces with biomolecules such as vitamin C.

Conclusions

In summary, we have designed and synthesized two novel hydroxy-functionalized polyaniline nanospheres to trace the molecular interaction at the nanosurfaces. We have successfully shown that the dihydroxy-functionalized aniline monomers can be synthesized via a tailor-made approach and polymerized to produce nanospheres with active hydrogen-bonding sites at the surfaces. The approach demonstrated here is very unique and highly novel: (i) two new hydroxyl-functionalized aniline molecules were synthesized for producing polyaniline nanospheres with active hydrogen-bonding groups at the surfaces, (ii) the hydroxyl functional groups enhance the solubility of the nanomaterials, allowing them to be characterized by NMR

spectroscopy, (iii) the mechanistic aspects of the polymerization were investigated by FT-IR and DLS studies, (iv) the hydroxyl-functionalized monomers undergo hydrogen-bonded aggregation in water to form 400–600 nm aggregates, and subsequent oxidations of these aggregates produce nanospheres rather than nanofibers (in the case of the unsubstituted monomer), (v) WXR studies give evidence of enhanced hydrogen-bonding interactions in the functionalized nanospheres with the appearance of a new peak at 13.4 Å, (vi) vitamin C was employed as an analyte to trace the molecular interactions at the polyaniline nanomaterial surface, and (vii) the nanospheres with bishydroxyl pendent at the surface show selective interactions with vitamin C and show enhanced sensing properties. The present approach clearly demonstrates the importance of nanosurface functionalization right from the synthesis to trace the sensing activity of biomolecules such as vitamin C.

Acknowledgment. We thank the Department of Science and Technology, New Delhi, India, for financial support under the NSTI scheme (Grant SR/S5/NM-06/2007). We thank Dr. Peter Koshy, Mr. M. R. Chandran, Dr. U. Syamaprasad, Mr. P. Gurusamy, and Dr. V. S. Prasad, NIIIST, Trivandrum, India, for SEM, WXR, and TEM analysis. We also thank Mr. Willi Paul, SCTIMST, Trivandrum, India, for dynamic light scattering analysis. P.A. thanks the UGC, New Delhi, India, for a senior research fellowship.

Supporting Information Available: ^1H NMR, ^{13}C NMR, and HR-MS spectra of the intermediate synthetic compounds, DLS plot of the An•HCl monomer and polymer nanospheres in water, FTIR spectra of the monomers and polymers, UV–vis–NIR absorption spectra of the polyaniline nanomaterials, and TGA data of the polymers. This information is available free of charge via the Internet at <http://pubs.acs.org>.

LA801128J